Letters

Decentralized Circulating Current Attenuation With Model Predictive Control for Distributed/Shunted Single/Three-Phase Grid-Tied Inverters

Liwei Zhou, *Student Member, IEEE*, and Matthias Preindl, *Senior Member, IEEE*

***Abstract*—This letter proposed a decentralized control method to attenuate the circulating current among the grid-connected inverters without extra cost on the communication. Based on the combination of cascaded model predictive control (MPC) and modified LCL filter topologies, the developed method can locally limit the circulating current for different types of inverters, e.g., single/three-phase grid-connection, and various applications, e.g., shunted or distributed inverters with/without common dc bus, respectively. The merits of the proposed method include the following. 1) Decentralized circulating current control without the need of a central controller or the corresponding communication to collect the sampling and calculate the common mode components for leakage current attenuation among different inverters. 2) Generalized control method that can be applied to single/three-phase inverters for both shunted and distributed inverters with/without common dc bus applications. 3) No synchronization is needed for pulsewidth modulation signals among different inverters to attenuate the circulating current. 4) Cascaded MPC without the need of individual inverter's grid side uncertain filter parameters for the attenuation of circulating current and system parametric modeling. 5) Better transient performance with the inner loop MPC. The experimental results verified the proposed method.**

***Index Terms*—Circulating current attenuation, decentralized control, distributed inverters, grid-connection, model predictive control (MPC), shunted inverters.**

I. Introduction

CIRCULATING current is a critical issue in the grid-connected inverters-interfaced renewable energy systems. The high frequency fluctuation of the common mode voltage in the inverters can generate leakage current to be flowing into the grid through the parasitic capacitance, especially in the photovoltaic (PV) stations. Traditionally, for the individual inverter, extra high/line frequency transformers or specially designed active bypassing circuits are needed to reduce the leakage current from flowing into the grid. Alternatively, in a centralized PV system with distributed inverters, the circulating leakage current can be attenuated by the synchronization of the pulse width modulation (PWM) carrier angles among the inverters. The latter method requires extra low latency communication channels which brings more cost. Also, for the shunted inverters that have common dc bus, there also exists circulating current among the parallel-connected inverters. In this case, a central controller is needed with the corresponding communication to the local controller of each shunted inverter to collect the sampling information and implement the circulating current control.

First, for the leakage current attenuation in individual grid-connected inverter, [1]–[8] proposed specially designed topologies with extra active bypassing circuits on ac and dc side. Specifically, the authors in [1]–[4] added the leakage current bypassing circuits on the ac side with extra freewheeling paths and the authors in [5]–[8] inserted the bypassing circuits on the dc side. Both methods induce extra device cost and power losses. Second, for the circulating current reduction among multiple grid-connected inverters, the applications can be divided into two types, distributed and shunted connections. The shunted inverters are connected in parallel with the common dc bus and the distributed inverters have the separate dc sources for each inverter. Wei *et al.* [9] proposed a circulating current reduction method for multiple shunted two-level inverters by gathering the leakage current of the local inverters into the central controller with communication. The authors in [10]–[14] developed different circulating current attenuation methods for shunted three-level three-phase inverters by leveraging a central controller to integrate the local inverters sampling information with communication. Zhang *et al.* [15] proposed another leakage current limiting technique for shunted three-level four-leg inverters. Zhang *et al.* [16] focused on the circulating current attenuation specifically for shunted single-phase inverters. Chen *et al.* [17] developed the circulating current mitigation methods for shunted three-level rectifiers system considering the neutral switching faults by leveraging communicated controllers among the converters. Zhang *et al.* [18] proposed to utilize the common-mode vectors to attenuate the resonance current among the shunted inverters with coordinated controllers. Li *et al.* [19] studied another method by modifying the three-level T-type shunted inverters with the communicated controllers to reduce the resonance circulating current. Li *et al.* [20] proposed an integrated modulation method to reduce the circulating current

Manuscript received March 2, 2022; revised April 21, 2022; accepted May 19, 2022. Date of publication May 30, 2022; date of current version June 24, 2022. This work was supported by NSF CAREER award under Grant 1653574. *(Corresponding author: Matthias Preindl.)*

The authors are with the Department of Electrical Engineering, Columbia University in the City of New York, New York, NY 10027 USA (e-mail: lz2575@columbia.edu; matthias.preindl@gmail.com).

Color versions of one or more figures in this article are available at https://doi.org/10.1109/TPEL.2022.3178931.

Digital Object Identifier 10.1109/TPEL.2022.3178931

and common-mode voltage for the shunted three-level inverters system with centralized control and PWM modulation strategies. Besides the shunted inverters, the circulating current reduction of distributed inverters with separate dc buses are also studied. For the distributed inverters system, since the inverters are distributed farther than the shunted inverters, the communication latency requirement is more critical. Bae and Kim and Quan and Li [21] and [22] proposed PWM synchronization-based methods to reduce the circulating current injection into the grid. Xu *et al.* [23] and [24] optimized the phase angles among the distributed inverters PWM signals with low latency communications. Ye *et al.* [25] proposed a circulating current attenuation method by evenly redistributing the active current and minimizing the reactive current among the distributed inverters with coordinated communications. Basu *et al.* and Song *et al.* [26] and [27] developed PWM synchronization methods to reduce the circulating current in parallel-connected motor traction inverters and grid-tied inverter, respectively. Thus, for the circulating current attenuation in shunted/distributed inverters systems, either central controllers or PWM synchronization requires low latency communication tools which bring extra complexity and cost.

This letter developed a decentralized control method to locally attenuate the circulating current based on cascaded model predictive control (MPC) and modified LCL filtering topology without extra cost on the communication. First, the control method combined with the modified filtering topology are demonstrated. Second, the applications of single/three-phase inverters for shunted and distributed grid-connected systems are illustrated. Finally, the experimental results verified the analysis.

II. Decentralized Circulating Current Control

The proposed decentralized circulating current control strategy for the modified three/single-phase inverters are shown in Fig. 1(a) and (b), respectively. For the modified LCL filtering topology of the inverters, the upper/lower output capacitors, C_{f+} and C_{f-}, are connected to the dc bus positive and negative terminals, respectively. This filtering circuitry modification contributes to bypassing the circulating leakage current without flowing into the grid. As are shown in Fig. 2(a) and (b) for the three/single-phase equivalent common mode circuits, the circulating current can be locally restricted within the switch side inductors and upper/lower output capacitors instead of flowing into the grid. In the equivalent circuits, the variables, $v_{x,\mathrm{abc},up}$ and $v_{x,\mathrm{abc},lo}$, represent switch legs upper and lower switch pulsating voltages, respectively. The attenuation of circulating current is achieved by combining the modified LCL filtering topology and the decentralized control strategy in Fig. 1. The main control architecture includes two cascaded loops: 1) outer loop grid side inductor dq current control for active/reactive power management and zero-sequence circulating current control for the attenuation of leakage current. The outer loop will generate the references for the per phase power module local MPC control; 2) inner loop per power module MPC to track the output capacitor voltage references from the outer loop and increase the control bandwidth.

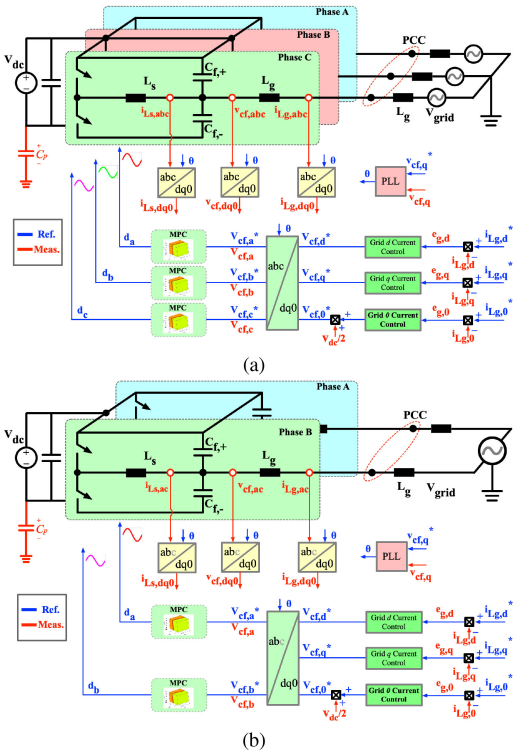

Fig. 1. Decentralized circulating current control strategies. (a) Three-phase. (b) Single-phase grid applications.

A. Outer Loop Circulating Current Control

For the outer loop control in Fig. 1(a) and (b), the grid side inductor dq current components and the circulating leakage current are controlled by PI with the references of $i^*_{Lg,d}$, $i^*_{Lg,q}$, and $i^*_{Lg,0}$, respectively. Specifically, the $i^*_{Lg,d}$ and $i^*_{Lg,q}$ are corresponding to the active and reactive power adjustments. And the outputs of grid side inductor dq current controllers are configured as the output capacitor dq voltage tracking references, $v^*_{Cf,d}$ and $v^*_{Cf,q}$, for the inner loop MPC control. For the decentralized attenuation of circulating current, $i^*_{Lg,0}$ is configured to be 0 A to restrict the leakage current from flowing into the grid and other inverters. Then, the output of decentralized circulating current controller will be superposed with half of dc bus voltage, v_{dc}, to formulate the zero-sequence output capacitor voltage tracking reference, $v^*_{Cf,0}$, for the inner loop MPC control. The Park/Clarke transformations are leveraged to transform the output capacitor references from $dq0$ to abc for three-phase application in Fig. 1(a) and to ab for single-phase application in Fig. 1(b).

B. Inner Loop Model Predictive Control

Each phase of the three/single-phase inverters is implementing the same MPC algorithm for the switch side LC filter to track the output capacitor voltage references, $v^*_{Cf,\mathrm{abc}}$ for three-phase and $v^*_{Cf,ab}$ for single-phase, received from the outer loop.

For the MPC implementation, in every control period, the MPC controller receives the measured switch side inductor current, $i_{Ls,\mathrm{abc}}$, capacitor voltage, $v_{Cf,\mathrm{abc}}$, grid current, $i_{Lg,\mathrm{abc}}$,

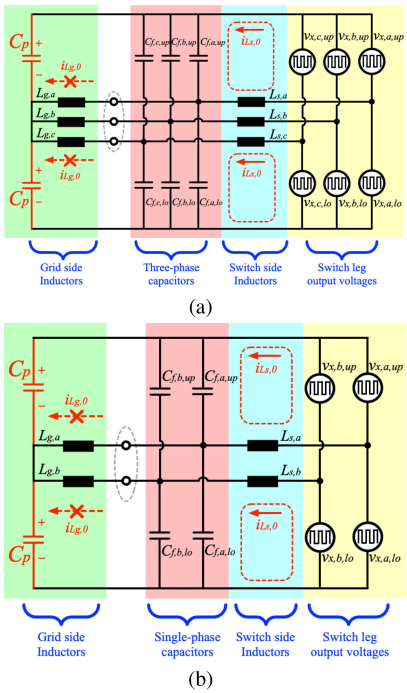

Fig. 2. Equivalent common mode circuits. (a) Three-phase. (b) Single-phase grid applications.

from analog-to-digital converter (ADC) and output capacitor voltage references, $v^*_{Cf,\text{abc}}$ from the outer loop controllers . An offline generated piecewise affine search tree is applied to derive the optimal duty cycle for the explicit MPC. The discrete state equations of switch side *LC* filter can be derived as follows:

$$i_{Ls}(k+1) = i_{Ls}(k) - \frac{T_s}{L_s} v_{Cf}(k) + \frac{v_{dc} T_s}{L_s} d(k) \tag{1a}$$

$$v_{Cf}(k+1) = \frac{T_s}{C_f} i_{Ls}(k) + v_{Cf}(k) - \frac{T_s}{C_f} i_{Lg}(k). \tag{1b}$$

For the flexibility of implementing the explicit MPC and the convenience of experimentally adjusting the dc bus voltage during test, the last term of (1), $v_{dc}d(k)$, can be replaced by the phase leg output voltage, $v_x(k)$. The state-space model for MPC can be expressed in standard matrix format of

$$X_{k+1} = A_C X_k + B_C u_k + E_C e_k \tag{2}$$

where the variables and matrices for MPC control represent

$$A_C = \begin{bmatrix} 1 & -\frac{T_s}{L_s} \\ \frac{T_s}{C_f} & 1 \end{bmatrix}, B_C = \begin{bmatrix} \frac{T_s}{L_s} \\ 0 \end{bmatrix}, E_C = \begin{bmatrix} 0 \\ -\frac{T_s}{C_f} \end{bmatrix} \tag{3a}$$

$$X_k = \begin{bmatrix} i_{Ls}(k) \\ v_{Cf}(k) \end{bmatrix}, u_k = \begin{bmatrix} v_{dc} d(k) \end{bmatrix}, e_k = \begin{bmatrix} i_{Lg}(k) \end{bmatrix}. \tag{3b}$$

In the MPC formulation, the inductor current/capacitor voltage references can be defined as $\bar{X}$ and the tracking errors between the measurement and the references are expressed as $\tilde{X}$ which are composed of

$$\bar{X}_k = \begin{bmatrix} i_{Ls,\text{ref}}(k) \\ v_{Cf,\text{ref}}(k) \end{bmatrix}, \tilde{X}_k = \begin{bmatrix} i_{Ls,\text{ref}}(k) - i_{Ls}(k) \\ v_{Cf,\text{ref}}(k) - v_{Cf}(k) \end{bmatrix}. \tag{4}$$

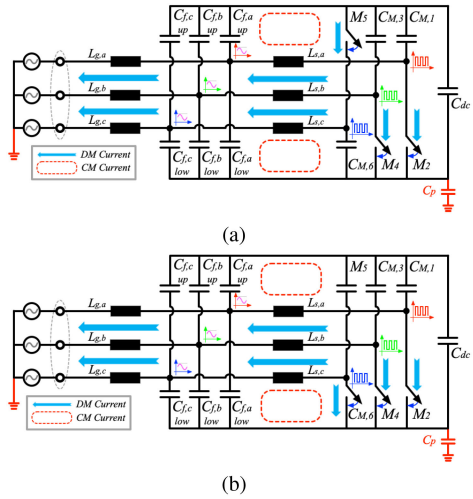

Fig. 3. Operation modes for three-phase modified inverter. (a) Active state. (b) Null state.

Thus, the cost function includes two terms

$$\min \sum_{k=0}^{N_c} \tilde{X}_k^T Q_C \tilde{X}_k + \sum_{k=0}^{N_p-1} \triangle u_k^T R_C \triangle u_k. \tag{5}$$

For the penalties of the MPC cost function, Q_C and R_C represent the weighing factor matrices that are implemented on the state values and input values, respectively.

The novelties of the developed control strategy can be concluded as: 1) The outer loop grid current $dq0$ components control for active/reactive power management and decentralized circulating current attenuation is cascaded with inner loop switch side inductor current, capacitor voltage model predictive control. The circulating current is restricted locally by the zero-sequence grid current controller in combination with the modified LCL circuit. The resonance are damped and control bandwidth are improved by the inner loop MPC. 2) The MPC is parameterized and implemented for the switch side inductor current, i_{Ls}, and output capacitor, v_{Cf}, instead of output side inductor. This control structure can avoid the inaccuracy and error caused by the modeling of grid side inductance uncertainty in the parameters. 3) The MPC is implemented in abc reference frame for per phase switch side LC filter. This implementation reduces the computation burden of the MPC algorithm generation and is flexible for random phase number in the single/three-phase grid applications.

C. Operation Modes

The operation modes of the modified three and single-phase grid-tied inverters are illustrated in Figs. 3 and 4, respectively. Specifically, Figs. 3(a) and 4(a) demonstrate the working modes in active states when the current is transferring between the dc and ac side through the upper and lower switches. Figs. 3(b) and 4(b) show the working modes in null states when the current is freewheeling through the lower switches. The blue arrows represent the differential mode (DM) current components and dashed red lines are the common mode (CM) current components.

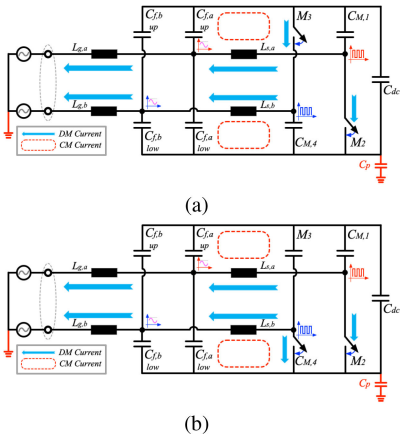

Fig. 4. Operation modes for single-phase modified inverter. (a) Active state. (b) Null state.

D. Circulating Current Suppression Principle

The circulating current suppression principle of the proposed method is mainly based on the combination of decentralized control strategies and the modified circuitry topologies in Fig. 1. First, the modified topologies in the filtering circuit provide a local circulating current bypassing path, as is shown in the red dashed lines in Figs. 2 and 3. This bypassing path itself has the partial capability of reducing the zero-sequence current by connecting the common points of output upper/lower capacitors to the positive/negative dc bus terminals. However, this connection modification can bypass 1/2 to 2/3 of the circulating current. Second, only applying the control method cannot attenuate the zero-sequence current, since the leakage current caused by the high-frequency CM noise on the switching side needs a physical path to flow through. Under this circumstance, the only path will be the grid side if no extra bypassing path is created. Finally, combining the decentralized circulating current control strategies and the modified circuitry topologies, the zero-sequence component of the duty cycle will prompt the circulating current to flow more through the upper/lower sides of bypassing circuits instead of the grid.

E. Capacitor and Inductor Design

The capacitor and inductor values design for the modified filtering circuit are analyzed in this subsection. The main standard that needs to follow is the grid current/voltage waveforms quality. The specification can be found from IEEE STD 519 to choose the value of grid side inductor, L_g, for the attenuation grid current harmonics.

For the switch side inductor, the minimum inductance, $L_{f,\min}$, can be determined by the maximum required current ripple, $\Delta i_{L,\max}$, with the duty cycle of 0.5, d, switching frequency, f_{sw}, and dc bus voltage, V_{dc}

$$L_{f,\min} = \frac{d(1-d)V_{dc}}{f_{sw}\Delta i_L}. \tag{6}$$

With the desired grid/switch side inductance determined, the capacitance can be designed by the minimum output voltage ripple, u_{ripple} and the resonant frequency of the LCL filter, ω_{res}. Specifically, the minimum capacitance is determined by the output voltage ripple which is expressed as

$$C_{f,up,\min} + C_{f,lo,\min} = \frac{1-d_{\min}}{8L_f u_{\text{ripple}}[\%] f_{sw}^2}. \tag{7}$$

Then, from the minimum available $C_{f,up,\min}$ and $C_{f,lo,\min}$, the value of capacitance can be adjusted to determine the resonant frequency of LCL filter system, as shown in

$$\omega_{res} = \sqrt{\frac{L_f + L_g}{L_f L_g (C_{f,up} + C_{f,lo})}}. \tag{8}$$

Based on (8), the capacitor values can be finally determined to choose a specific resonant frequency of the LCL filter. Then, with the help of ω_{res} and LCL parameters, the control bandwidth, ω_c, can be further designed to avoid the excitation.

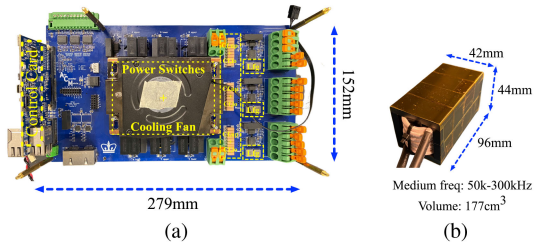

Fig. 5. Prototype of (a) the inverter board and (b) switch side inductor.

Fig. 6. Experimental prototype.

III. Merits and Validations

The merits of the developed decentralized circulating current control are validated in this section. Fig. 5 shows the prototype of inverter board and the switch side inductor. The power switches are cooled with fan on the top. The output capacitors, TDK FA10 ceramic capacitors, and grid side surface mount inductors are all integrated on the inverter board. The total volume of the inversion system is 2.38 L including 1.85 L of the inverter board and 0.53 L of the switch side inductors. The existing bypassing circuit solutions cost extra active switches than the proposed methods. Guo *et al.* [3] and [4] of the ac bypassing solutions cost 6 and 2 more switches than the proposed method. Guo *et al.* and Freddy *et al.* [7] and [8] of the dc bypassing solutions cost 2 and 1 more switches than the proposed method. Fig. 6 shows the prototype of three separate inverter boards, three sets of

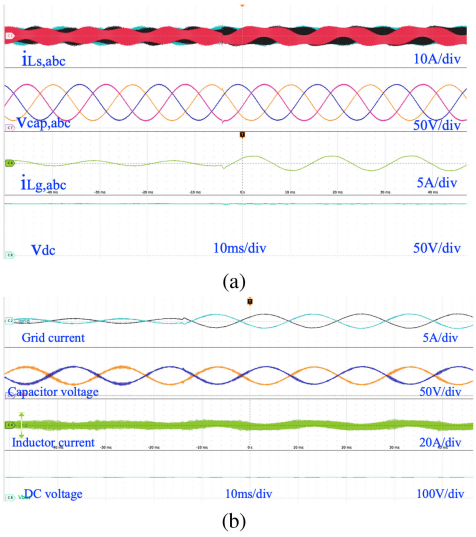

Fig. 7. Switch side inductor current, output capacitor voltage, grid side inductor current, and dc bus voltage transient waveforms for (a) three-phase and (b) single-phase grid applications with a current step of 4 A.

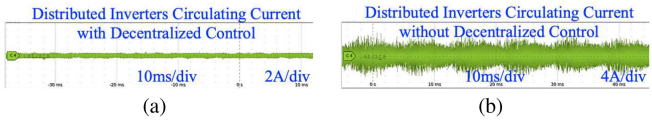

Fig. 8. Circulating current comparison for distributed inverters not sharing the same dc bus (a) with and (b) without the developed control strategy during transient.

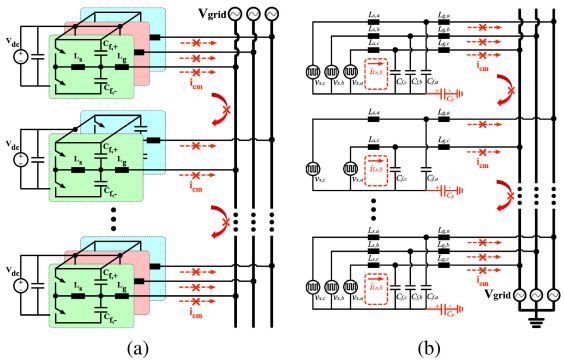

Fig. 9. (a) Distributed grid-connected inverters structure without common dc bus and (b) the corresponding equivalent common mode circuits.

three-phase switch side inductors, inverter board power supplies, three dc power supplies for the distributed inverters and scope. Fig. 7(a) and (b) show the switch side inductor current, output capacitor voltage, grid side inductor current, and dc voltage waveforms for three/single-phase grid-connected inverters, respectively, with a current step of 4 A. Fig. 8(a) and (b) compares the circulating current between with and without the decentralized control method among distributed inverters in Fig. 9 with separate dc bus during the current step transient period. The developed local circulating current attenuation method reduces the leakage current by a factor 6. Fig. 10(a) and (b) compares the circulating current between with and without the decentralized

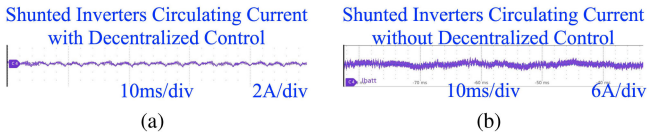

Fig. 10. Circulating current comparison for shunted inverters sharing the same dc bus (a) with and (b) without the developed control strategy during transient.

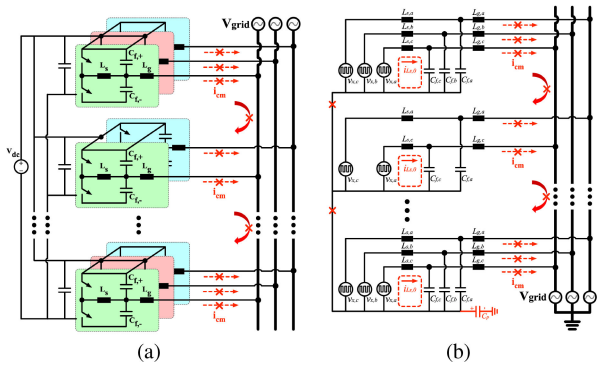

Fig. 11. (a) Shunted grid-connected inverters structure with common dc bus and (b) the corresponding equivalent common mode circuits.

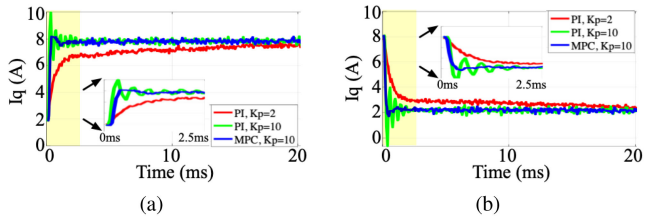

Fig. 12. Experimental transient comparison of conventional PI and developed MPC with current steps from (a) 2 to 8 A and (b) 8 to 2 A.

control method among shunted inverters in Fig. 11 with common dc bus during the current step transient period. The dc offset and ripple of the circulating current are reduced by a factor of 5. For the validation of transient performance improvement of the cascaded MPC, the comparison between the developed control and conventional PI are shown in Fig. 12(b) and (a) with current steps from 2 to 8 A and 8 to 2 A, respectively. The inner loop MPC enables a larger control gain for the outer loop PI with higher control bandwidth, faster reference tracking, and less oscillation during transients. The rising time of cascaded MPC is less than 1.5 ms without oscillation at a gain of 10. However, the conventional PI can only perform stably at a low gain of 2. A same high gain of 10 as the MPC will result in big oscillation for the conventional PI during transient. Thus, the cascaded MPC of the developed decentralized circulating current control improves the dynamic performance without the need/influence of grid side inductance parameters. Also, no communication channels are needed for central controller in [9]–[16] or PWM synchronization in [21]–[24].

For the contributions of this letter, we have concluded the following aspects. First, a decentralized circulating current control

is developed without the need of a central controller or the corresponding communication to collect the sampling for leakage current attenuation among different inverters. Second, the control method is suitable for both single/three-phase inverters under shunted or distributed connections with/without common dc bus applications. Third, no synchronization is needed for PWM signals among different inverters to attenuate the circulating current. Fourth, cascaded inner loop MPC control structure improves the modeling accuracy without the need of the individual inverter's grid side uncertain filter parameters for the attenuation of circulating current and system parametric modeling. Finally, the transient performance and control bandwidth are improved with MPC.

IV. Conclusion

This letter developed a decentralized circulating current control method based on the combination of cascaded MPC and modified LCL filtering topology. The control strategies can be applied locally to attenuate the circulating leakage current among the grid-connected inverters in distributed areas without common dc bus or shunted connection with common dc bus. Both single/three-phase inverters can leverage the control architecture to restrict the leakage current. Compared to the conventional circulating current attenuation methods, no communication tools are needed to either gather the local inverters sampling information or synchronize the PWM signals among the local inverters for a centralized circulating current elimination. Thus, the communication cost is largely reduced. Also, the local cascaded MPC avoids needing the various individual inverters grid side filter parameter information. The dynamic performance is improved with the inner loop MPC.

References

[1] H. F. Xiao, K. Lan, and L. Zhang, "A quasi-unipolar SPWM full-bridge transformerless PV grid-connected inverter with constant common-mode voltage," *IEEE Trans. Power Electron.*, vol. 30, no. 6, pp. 3122–3132, 2015.

[2] T. Kerekes, R. Teodorescu, P. Rodríguez, G. Vázquez, and E. Aldabas, "A new high-efficiency single-phase transformerless PV inverter topology," *IEEE Trans. Ind. Electron.*, vol. 58, no. 1, pp. 184–191, 2011.

[3] X. Guo, Y. Yang, and T. Zhu, "Esi: A novel three-phase inverter with leakage current attenuation for transformerless PV systems," *IEEE Trans. Ind. Electron.*, vol. 65, no. 4, pp. 2967–2974, 2018.

[4] X. Guo, R. He, J. Jian, Z. Lu, X. Sun, and J. M. Guerrero, "Leakage current elimination of four-leg inverter for transformerless three-phase pv systems," *IEEE Trans. Power Electron.*, vol. 31, no. 3, pp. 1841–1846, 2016.

[5] R. Gonzalez, J. Lopez, P. Sanchis, and L. Marroyo, "Transformerless inverter for single-phase photovoltaic systems," *IEEE Trans. Power Electron.*, vol. 22, no. 2, pp. 693–697, 2007.

[6] B. Yang, W. Li, Y. Gu, W. Cui, and X. He, "Improved transformerless inverter with common-mode leakage current elimination for a photovoltaic grid-connected power system," *IEEE Trans. Power Electron.*, vol. 27, no. 2, pp. 752–762, 2012.

[7] X. Guo, N. Wang, B. Wang, Z. Lu, and F. Blaabjerg, "Evaluation of three-phase transformerless DC-bypass PV inverters for leakage current reduction," *IEEE Trans. Power Electron.*, vol. 35, no. 6, pp. 5918–5927, 2020.

[8] T. K. S. Freddy, N. A. Rahim, W.-P. Hew, and H. S. Che, "Modulation techniques to reduce leakage current in three-phase transformerless h7 photovoltaic inverter," *IEEE Trans. Ind. Electron.*, vol. 62, no. 1, pp. 322–331, 2015.

[9] B. Wei, J. M. Guerrero, J. C. Vásquez, and X. Guo, "A circulating-current suppression method for parallel-connected voltage-source inverters with common dc and ac buses," *IEEE Trans. Ind. Appl.*, vol. 53, no. 4, pp. 3758–3769, 2017.

[10] Y. Fu, N. Cui, Z. Chen, and C. Zhang, "An improved finite-time control strategy for zero-sequence circulating current suppression of parallel three-level rectifiers," *IEEE Trans. Emerg. Sel. Topics Power Electron.*, vol. 8, no. 4, pp. 3933–3943, 2020.

[11] C. Qin, C. Zhang, A. Chen, X. Xing, and G. Zhang, "Circulating current suppression for parallel three-level inverters under unbalanced operating conditions," *IEEE Trans. Emerg. Sel. Topics Power Electron.*, vol. 7, no. 1, pp. 480–492, 2019.

[12] A. Chen, Z. Zhang, X. Xing, K. Li, C. Du, and C. Zhang, "Modeling and suppression of circulating currents for multi-paralleled three-level t-type inverters," *IEEE Trans. Ind. Appl.*, vol. 55, no. 4, pp. 3978–3988, 2019.

[13] X. Xing, X. Li, C. Qin, J. Chen, and C. Zhang, "An optimized zero-sequence voltage injection method for eliminating circulating current and reducing common mode voltage of parallel-connected three-level converters," *IEEE Trans. Ind. Electron.*, vol. 67, no. 8, pp. 6583–6596, 2020.

[14] X. Xing, C. Zhang, A. Chen, H. Geng, and C. Qin, "Deadbeat control strategy for circulating current suppression in multiparalleled three-level inverters," *IEEE Trans. Ind. Electron.*, vol. 65, no. 8, pp. 6239–6249, 2018.

[15] C. Zhang, R. Zhang, X. Xing, and X. Li, "Circulating current mitigation and harmonic current compensation for multi-function parallel three-level four-leg converters," *IEEE Trans. Emerg. Sel. Topics Power Electron.*, to be published, doi: 10.1109/JESTPE.2021.3072437.

[16] C. Zhang, Z. Wang, X. Xing, X. Li, and X. Liu, "Modelling and suppression of circulating currents among parallel single-phase three-level transformerless grid-tied inverters," *IEEE Trans. Ind. Electron.*, to be published, doi: 10.1109/TIE.2021.3127012.

[17] Z. Chen, X. Xing, X. Li, X. Pang, and C. Zhang, "The zero-sequence circulating current suppression method for parallel three-level rectifiers system under the open circuit fault of neutral-point switches," *IEEE Trans. Ind. Inform.*, to be published, doi: 10.1109/TII.2022.3157331.

[18] C. Zhang, X. Li, X. Xing, B. Zhang, R. Zhang, and B. Duan, "Modeling and mitigation of resonance current for modified LCL-type parallel inverters with inverter-side current control," *IEEE Trans. Ind. Inform.*, vol. 18, no. 2, pp. 932–942, 2022.

[19] X. Li, X. Xing, C. Qin, C. Zhang, and G. Zhang, "Design and control method to suppress resonance circulating current for parallel three-level rectifiers with modified LCL filter," *IEEE Trans. Ind. Electron.*, vol. 68, no. 8, pp. 7012–7023, 2021.

[20] W. Li *et al.*, "Integrated modulation of dual-parallel three-level inverters with reduced common mode voltage and circulating current," *IEEE Trans. Power Electron.*, vol. 36, no. 11, pp. 13332–13344, 2021.

[21] Y. Bae and R.-Y. Kim, "Suppression of common-mode voltage using a multicentral photovoltaic inverter topology with synchronized pwm," *IEEE Trans. Ind. Electron.*, vol. 61, no. 9, pp. 4722–4733, 2014.

[22] Z. Quan and Y. W. Li, "Suppressing zero-sequence circulating current of modular interleaved three-phase converters using carrier phase shift pwm," *IEEE Trans. Ind. Appl.*, vol. 53, no. 4, pp. 3782–3792, 2017.

[23] T. Xu *et al.*, "Two-layer global synchronous pulse width modulation method for attenuating circulating leakage current in pv station," *IEEE Trans. Ind. Electron.*, vol. 65, no. 10, pp. 8005–8017, 2018.

[24] T. Xu, F. Gao, K. Zhou, P. Tan, C. Zhang, and E. Chi, "A min–max closed-loop PLL-GSPWM for circulating leakage currents attenuation in PV station," *IEEE Trans. Power Electron.*, vol. 36, no. 9, pp. 10224–10238, 2021.

[25] Z. Ye, P. K. Jain, and P. C. Sen, "Circulating current minimization in high-frequency AC power distribution architecture with multiple inverter modules operated in parallel," *IEEE Trans. Ind. Electron.*, vol. 54, no. 5, pp. 2673–2687, 2007.

[26] K. Basu, J. S. S. Prasad, and G. Narayanan, "Minimization of torque ripple in PWM AC drives," *IEEE Trans. Ind. Electron.*, vol. 56, no. 2, pp. 553–558, 2009.

[27] C. Song, R. Zhao, M. Zhu, and Z. Zeng, "Operation method for parallel inverter system with common dc link," *IET Power Electron.*, vol. 7, no. 5, pp. 1138–1147, 2014.